Fingerprint Matching Using Hierarchical Level Features

D. Bennet [1], Dr. S. Arumuga Perumal [2]
1 Assistant Professor & Scholar, Department of Computer Science, S.T. Hindu College, Nagercoil, India.
2 Associate Professor & Head, Department of Computer Science, S.T. Hindu College, Nagercoil, India

Abstract - **This paper proposes a fingerprint features extraction using different levels. The hierarchical order at four different levels, namely, Level 1 (pattern), Level 2 (minutia points), Level 3 (pores and ridge contours), and Level 4 (oscillated pattern). The fingerprint feature extraction frequently take advantage of Level 4 features to assist in identification, Automated Fingerprint Identification Systems (AFIS) currently rely only on Level 1 and Level 2 features. In fact, the Federal Bureau of Investigation's (FBI) standard of fingerprint resolution for AFIS is 500 pixels per inch (ppi), which is inadequate for capturing Level 3 features, such as pores. With the advances in fingerprint sensing technology, many sensors are now equipped with dual resolution (1,000 ppi) scanning capability. However, increasing the scan resolution alone does not necessarily provide any performance improvement in fingerprint matching, unless an extended feature set is utilized. As a result, a systematic analysis to determine how much performance gain one can achieve by introducing Level 4 features in AFIS is highly desired. We propose a hierarchical matching system that utilizes features at all the four levels extracted from 1,000-ppi fingerprints scans. Level 3 features, pores and ridge contours are automatically extracted using Gabor filters and wavelet transform and are locally matched using the Iterative Closest Point (ICP) algorithm and Level 4 features, oscillated pattern including curve scanned DCT to measure the recognition rate using *k-nn* classifier, Our analytical study conclude Level 4 features carry significant discriminatory information. The matching system when Level 4 features are employed in combination with Level 1 Level 2 and Level 3 features. This proposed method outperforms the others, particularly in recognition rate.**

Keywords - **Fingerprint features, minutia, Level features, extended feature set, pores, ridge contours, oscillated pattern, curve-DCT, hierarchical matching.**

I. INTRODUCTION

Fingerprint based biometric systems are rapidly gaining acceptance as one of the most effective technologies to authenticate users in a wide range of applications. In fingerprint identification is based on two properties, namely, uniqueness and permanence.

The fingerprint features are generally categorized into four levels. Level1 features, or patterns, are the macro details of the fingerprint such as ridge flow and pattern type. Level 2 features, or minutiae, such as ridge bifurcations and endings. Level 3 features, or shape, include all dimensional attributes of the ridge such as ridge path deviation, width, shape, pores, edge contour, incipient ridges, breaks, creases, scars, and Level 4 or oscillated pattern curve scanned DCT.

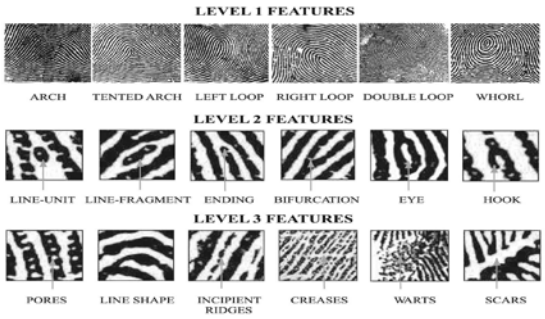

LEVEL 4 FEATURES

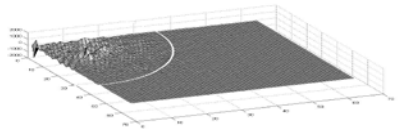

Fig.1 Fingerprint features at Level 1, Level 2, Level 3 and Level 4

Fig.1 Shown that Level 1 features, though not unique, are useful for fingerprint classification (e.g., into whorl, left loop, right loop, and arch classes), while Level 2 features have sufficient discriminating power to establish the individuality of fingerprints. Similarly, Level 3 features are also claimed to be permanent, immutable, and unique according to the forensic experts, and Level 4 features if properly utilized, can provide discriminatory information for human identification [3]. Both Level 3 and Level 4 features play important roles in providing quantitative as well as qualitative information for identification

II.HISTORY

Fingerprints as a scientific method for identification traces back to the 1880s, when Faulds suggested that latent fingerprints obtained

at crime scenes could provide knowledge about the identity of offenders [4]. In 1892, Galton introduced Level 2 features by defining minutia points as either ridge endings or ridge bifurcations on a local ridge. In 1912, Locard introduced the science of poroscopy, the comparison of sweat pores for the purpose of personal identification.

In 1962, Chatterjee discovered that some shapes on the friction ridge edges tend to reappear frequently and classified them into eight categories, namely, straight, convex, peak, table, pocket, concave, angle, and others (see Fig. 2).

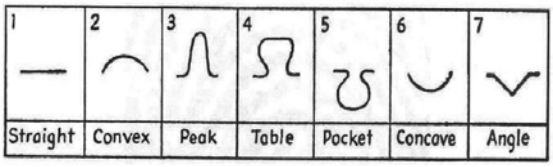

Fig. 2 Characteristic features of friction ridges

It is believed that the differences in edge shapes are caused by the effects of differential growth on the ridge itself or a pore that is located near the edge of the friction ridge.

A. Fingerprint Formation

Human fingers are known to display friction ridge skin (FRS) that consists of a series of ridges and furrows, generally referred to as fingerprints. The FRS is made of two major layers: dermis (inner layer) and epidermis (outer layer). Pores, on the other hand, penetrate into the dermis starting from the epidermis. Each ridge unit contains one sweat gland, pores are often considered evenly distributed along ridges and the spatial distance between pores frequently appears to be in proportion to the breadth of the ridge, which, on an average, is approximately 0.48 mm. A pore can be visualized as either open or closed in a fingerprint image based on its perspiration activity. A closed pore is entirely enclosed by a ridge, while an open pore intersects with the valley lying between two ridges (see Fig. 3).

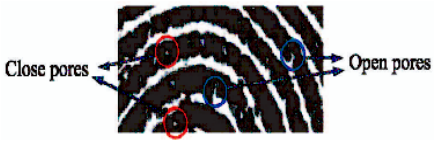

Fig. 3 Open and closed pores

One should not expect to find two separate prints of the same pore to be exactly alike, as a pore may be open in one and closed in the other print.

B. Fingerprint Sensing Technology

There are many different sensing methods to obtain the ridge-and-valley pattern of finger skin or fingerprint [10]. Historically, in law enforcement applications, fingerprints were mainly acquired offline. Nowadays, most commercial and forensic applications accept live-scan digital images acquired by directly sensing the finger surface with a fingerprint sensor based on optical, solid-state, ultrasonic, and other imaging technologies.

Direct sensing of fingerprints as electronic signals started with optical "live-scan" sensors with Frustrated Total Internal Reflection (FTIR) principle. When the finger touches the top side of a glass prism, one side of the prism is illuminated through a diffused light. While the fingerprint valleys that do not touch the glass platen reflect the light, ridges that touch the platen absorb the light. This differential property of light reflection allows the ridges (which appear dark) to be discriminated from the valleys. Solid-state fingerprint sensing technique uses silicon based, direct contact sensors to convert the physical information of a fingerprint into electrical signals.

New fingerprint sensing technologies MSI (Multispectral Fingerprint Imaging) technology appear to be of significantly better quality compared to conventional optical sensors for dry and wet fingers. One of the most essential characteristics of a digital fingerprint image is its resolution, which indicates the number of dots or pixels per inch (ppi) (see Fig. 4).

Fig. 4 Fingerprint resolution same fingerprint captured at different image resolutions
(a) 380 ppi (b) 500 ppi and (c) 1,000 ppi

III. PREVIOUS WORKS

Only a few researchers have studied the use of Level 3 features in an automated fingerprint identification system. Skeletonization - based pore extraction and matching algorithm [6]. Specifically, the locations of all end points (with at most one neighbor) and branch points (with exactly three neighbors) in the skeleton image are extracted and each end point is used as a starting location for tracking the skeleton. The tracking algorithm advances one element at a

time until one of the following stopping criteria is encountered: 1) another end point is detected, 2) a branch point is detected, and 3) the path length exceeds a maximum allowed value. Condition 1) implies that the tracked segment is a closed pore, while Condition 2) implies an open pore. Finally, skeleton artifacts resulting from scars and wrinkles are corrected and pores from reconnected skeletons are removed. The result of pore extraction is shown in Fig. 5.

Fig.5 Pore detection based on skeletonization (a) Fingerprint detected pores. (b) The raw skeleton image

During matching, score between a given image pair is then defined as a ratio of the number of matched pores to the total number of pores extracted from template regions,

1. Skeletonization is effective for pore extraction only when the image quality is very good.
2. Comparison of small fingerprint regions based on the distribution of pores.ments.
3. The alignment of the test and the query region is established based on intensity correlation, which is computationally expensive by searching through all possible rotations and displacements.
4.

IV. LEVEL3 FEATURE EXTRACTIONS

As suggested in [7], Level 1, Level 2, and Level 3 features in a fingerprint image are mutually correlated. Based on the physiology of the fingerprint, pores are only present on the ridges, not in the valleys. During image acquisition, we observe that the ridge contour is often more reliably preserved at 1,000 ppi than the pores, especially in the presence of various skin conditions and sensor noise (see Fig. 6).

Fig. 6 Two impressions of the same finger at 1,000 ppi

In order to automatically extract Level 3 features, namely, pores and ridge contours, we have developed feature extraction algorithms using Gabor filters and wavelet transform.

A. Pore Detection

Based on their positions on the ridges, pores can be divided into two categories: open and closed. A closed pore is entirely enclosed by a ridge, while an open pore intersects with the valley lying between the two ridges.

To enhance the ridges, we use Gabor filters, which has the form

$$G(x, y : \theta, f) = \exp\{-\frac{1}{2}[x\frac{x_\theta^2}{\delta_x^2} + \frac{y_\theta^2}{\delta_y^2}]\cos(2\pi f x\theta\}$$

Where θ and f are the orientation and frequency of the filter, respectively, θ x and θ y are the standard deviations of the Gaussian envelope along the x- and y-axes, respectively. Here, (x θ; y θ) represents the position of a point (x, y) after it has undergone a clockwise rotation by an angle (90^o - θ). The four parameters of the Gabor filter are (θ ,f, δ_x , δ_y)ridge frequency and orientation .

B. Ridge Contour Extraction

The ridge contour is defined as edges of a ridge. However, the flexibility of the friction skin and the presence of open pores tend to reduce the reliability of ridge edge classification. In contrast to edgeoscopy, our method utilizes the ridge contour directly as a spatial attribute of the ridge and the matching is based on the spatial distance between points on the ridge contours.

Fig. 7 Ridge contour extraction.
(a) Wavelet (b) Ridge contour (c) Gabor

Classical edge detection algorithms can be applied to fingerprint images to extract the ridge contours. However, the detected edges are often very noisy due to the sensitivity of the edge detector to the presence of creases and pores. Hence, we again use wavelets to enhance the ridge contours and linearly combine them with a Gabor enhanced image (where broken ridges are fixed) to obtain enhanced ridge contours.

V. LEVEL 4 FEATURE EXTRACTIONS

The informative features extraction method is curve-scanned DCT. The extracted features can subsequently be used for fingerprint

matching process. The curve-scanned DCT coefficients have a high matching score and also its evaluated by the *k*-nearest neighbor (*k*-NN) classifier and the time required in the processing steps are compared.

However, we found that the informative features used for matching purpose exist within the low frequency area (top-left corner) of the distribution plane only. From our observation, magnitude of most features extracted from the middle and high frequency areas (around 75%) of DCT coefficients, from different fingerprint images, are hardly changed. Hence, we bound the energy compactness area to be used for creating the fingerprint features by a white arch as shown in Fig.8. This boundary is actually defined by the oscillated pattern contained within the top-left corner of the distribution plane of the DCT coefficients, which disperses equally in all directions from the DC component. The DCT coefficients divided in this fashion are thus referred to as curve-scanned DCT coefficients. Note that the area within the boundary is approximately 25% of the distribution plane.

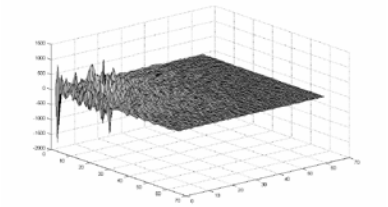

Fig. 8: DCT coefficients distributions

To generate the fingerprint features from the curve-scanned DCT coefficients, firstly we cropped a gray-scale fingerprint image to the size of 64×64 pixels, where the reference point was at the center of the cropped image. Secondly, the cropped image was quartered to obtain four non-overlapping images of size 32×32 pixels. Then, the DCT was applied to each non-overlapping image. The DCT coefficients within the boundary were divided into 5 areas in the curve-scanned fashion, where each area was 2-pixel width (see Fig. 9)

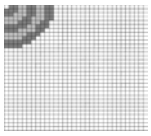

Fig.9 Curve-scanned DCT coefficients

Finally, the standard deviation of the DCT coefficients in each area from all 4 non-overlapping images was computed to create a feature vector of the length 20 (5 features from each non-overlapping image). The performance indicator we used to evaluate our proposed method was the recognition rate obtained from the *k* nearest neighbors (*k*-NN) classifier with no rejection option. Recall that, in *k*-NN classifier, the database is divided into 2 data sets, namely training set and testing set. Basically, training set is a set of fingerprint images stored in a fingerprint image database, while testing set is a set of entry fingerprint images. Hence, *k* nearest neighbor is merely *k* instances in the training set, which nearest to the testing set, and nearest neighbor is evaluated by the distance between both sets. The nearest neighbors of an instance are normally defined in term of the standard Euclidean distance [1]. Given *xi* and *xj* are the feature vectors from the training sets and testing sets, respectively, the distance between two feature vectors is then defined to be *d* (*xi*, *xj*), where

$$d(x_i, x_j) = \sqrt{\sum_{r=1}^{n} (x_i - x_j)^2}$$

For the complexity indicator, we measured the processing time required in the features extraction process and the fingerprint matching process. This can be easily achieved by timing such processes.

VI. HIERARCHICAL MATCHING

Fig. 10 illustrates the architectural design of our proposed matching system. Each layer in the system utilizes features at the corresponding level.

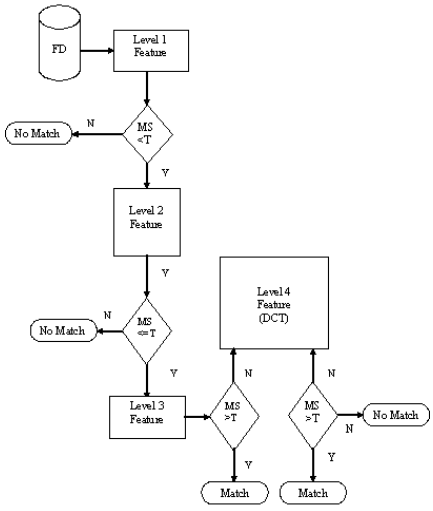

Fig.10 Hierarchical matching system flow chart

In general, the numbers of impostor minutia matches decreases after Level 3 features are used, while the number of genuine minutia

Matches remain almost unchanged. As a result, the overlap region of the genuine and impostor distributions of matched minutiae is reduced after Level 3 features were utilized. Although the latter is a more commonly used and straight-forward approach, it is more time-consuming since matching at both Level 2 and Level 3 has to be performed for every query. In addition, parallel score fusion is sensitive to the selected normalization scheme and fusion rule. On the other hand, the proposed hierarchical matcher enables us to control the level of information or features to be used at different stages of fingerprint matching.

VII. EXPERIMENTAL RESULTS

In general, our experiments show significant performance improvement when we combine Level 3 and Level 4 features in a hierarchical fashion. It is demonstrated that Level 3 features do provide additional discriminative information and should be used in combination with Level 2 features. The results of this study strongly suggest that using Level 4 features in fingerprint matching at 1,000 ppi is both practical and beneficial.

VIII. SUMMARY AND CONCLUSIONS

We conclude that the fingerprint feature extraction scheme for hierarchal levels the variation in matching score is presented as a Table and graph below.

Table.1 matching score

Diff. Levels	Matching Score
Level 1	65
Level 2	84
Level 3	92
Level 4	97

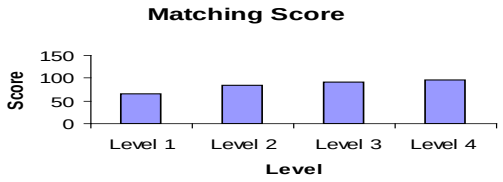

Fig.11 Matching score presentation

To obtain the discriminatory information at level 4 we introduced. The algorithm based on curve – scanned DCT to automatically extract maximum features. In our analytical results strongly proposed Level 4 feature extraction is high matching score and improve the recognition rate.

REFERENCES

[1] S. Tachaphetpiboon, “Fingerprint Features Extraction Using Curve-scanned DCT Coefficients” 1-4244-1374-5/07@2007 IEEE
[2] F. Galton, “Personal Identification and Description,” Nature, vol. 38, pp. 201-202, 1888.
[3] H. Cummins and M. Midlo, Finger Prints, Palms and Soles: An Introduction to Dermatoglyphics. Dover, 1961.
[4] S. Pankanti, S. Prabhakar, and A.K. Jain, “On the Individuality of Fingerprints,” IEEE Trans. Pattern Analysis and Machine Intelligence, vol. 24, no. 8, pp. 1010-1025, Aug. 2002.
[5] J.D. Stosz and L.A. Alyea, “Automated System for Fingerprint Authentication Using Pores and Ridge Structure,” Proc. SPIE Conf. Automatic Systems for the Identification and Inspection of Humans, vol. 2277, pp. 210-223, 1994.
[6] R. McCabe and M. Garris, “Summary of April 2005 ANSI/NIST Fingerprint Standard Update Workshop,” http://fingerprint.nist.gov/standard/, 2005
[7] Anil k. Janin, “Pores and Ridges: High Resolution Fingerprint Using Level 3 Features”, IEEE vol.29 No.1 2007.
[8] S. Meagher and A. Hicklin, “Extended Fingerprint Feature Set,” Proc. ANSI/NIST ITL 1-2000 Standard Update Workshop, 2005.
[12 A.K. Jain, S. Prabhakar, and S. Chen, “Combining Multiple Matchers for a High Security Fingerprint Verification System,” Pattern Recognition Letters, vol. 20, nos. 11-13, pp. 1371-1379, 1999
[9] P.J. Besl and N.D. McKay, “A Method for Registration of 3D Shapes,” IEEE Trans. Pattern Analysis and Machine Intelligence, vol. 14, no. 2, pp. 239-256, Feb. 1992.
[10] A. Ross, S.C. Dass, and A.K. Jain, “Fingerprint Warping Using Ridge Curve Correspondences,” IEEE Trans. Pattern Analysis and Machine Intelligence, vol. 28, no. 1, pp. 19-30, Jan. 2006.
[11] A.K. Jain, Y. Chen, and M. Demirkus, “Pores and Ridges: Fingerprint Matching Using Level 3 Features,” Proc. Int’l Conf. Pattern Recognition, vol. 4, pp. 477-480 Aug. 2006.
[12] Y. Chen, S.C. Dass, and A.K. Jain, “Fingerprint Quality Indices for Predicting Authentication Performance,” Proc. Audio- and Video- Based Biometric Person Authentication, pp. 160-170, 2005.